scientific reports

Check for updates

OPEN

The complete mitogenome of Amazonian *Brachyplatystoma filamentosum* and the evolutionary history of body size in the order Siluriformes

Renata Lilian Dantas Cavalcante[1], Caio Santos Silva[2], Amanda Ferreira Vidal[3], Éder Soares Pires[3], Gisele Lopes Nunes[3], Luciano Fogaça de Assis Montag[4], Guilherme Oliveira[3], Ândrea Ribeiro-dos-Santos[2], Sidney Santos[2], Sandro José de Souza[1,5,6], Jorge Estefano de Santana Souza[1] & Tetsu Sakamoto[1]✉

The order Siluriformes (catfish) is one of the largest groups of fish. Diversity in the body size among its species, which range from a few centimeters to 4 meters, makes Siluriformes an interesting group to investigate the body size evolution. Here, we present the complete mitogenome of *Brachyplatystoma filamentosum* (Piraíba), the largest Amazonian catfish, to explore the evolutionary history of Siluriformes and their body size dynamics. The Piraíba's mtDNA is 16,566 bp long, with a GC content of 42.21% and a D-loop of 911 bp. Phylogenetic analysis was conducted using protein-coding sequences, tRNAs, and rRNAs from mtDNA of Piraíba and 137 other Siluriformes species. Time-calibrated maximum likelihood trees estimated the origin of the order Siluriformes to be ~118.4 Ma, with the Loricarioidei suborder diversifying first, followed by Diplomystoidei and Siluroidei. The Siluroidei suborder experienced rapid expansion around 94.1 Ma. Evolutionary dynamics revealed 16 positive and 11 negative directional body size changes in Siluriformes, with no global trend toward larger or smaller sizes, and with Piraíba showing a significant size increase (5.65 times over 40.8 Ma). We discuss how biological, ecological and environmental factors could have shaped the evolution of body size in this group.

Keywords Catfish, Mitogenome, Phylogenetics, Evolution, Gigantism, Amazon

The Siluriformes order, commonly referred to as catfish, constitutes one of the most extensive and diverse natural groups of freshwater teleost fish[1]. With a staggering array of more than 3,900 recognized species, Siluriformes inhabit a wide spectrum of aquatic environments globally. These encompass rivers, lakes, swamps, and certain species that display an ability to endure salinity levels akin to estuarine or even oceanic conditions[2]. Manifesting an extraordinary range of shapes and sizes, the catfish order includes diminutive species measuring just a few centimeters in length, such as the *Corydoras panda* (∼ 3.8 cm), in stark contrast to the colossal counterparts like the *Brachyplatystoma filamentosum* (∼ 360 cm)[3].

The diversity in the body size found among species from Siluriformes makes them an interesting group to understand the evolutionary dynamics of this trait. Body size is a trait that affects important aspects of the organism's biology, such as fitness, behavior, fecundity, longevity, and susceptibility to diseases, such as cancer[4]. Due to its impact on our understanding of life, several efforts were made to uncover general patterns of body size evolution in different taxonomic groups, including cetaceans[5,6], carnivores[7,8], mammals in general[9], reptiles[10–13], and insects[14]. Some rules that guide the evolution of body size proposed are Cope's rule[15,16], which describes a

[1]Bioinformatics Multidisciplinary Environment/BioME, IMD, Federal University of Rio Grande do Norte, Natal, RN 59078-900, Brazil. [2]Laboratory of Human and Medical Genetics, Institute of Biological Sciences, Federal University of Pará, Belém, PA 66075-110, Brazil. [3]Vale Institute of Technology, Belém, PA 66055-090, Brazil. [4]Laboratory of Ecology and Conservation, Institute of Biological Sciences, Federal University of Pará, Belém, PA 66075-110, Brazil. [5]Brain Institute, Federal University of Rio Grande do Norte, Natal, RN 59078-970, Brazil. [6]DNA-GTX Bioinformatics, Natal, RN, Brazil. ✉email: tetsu@imd.ufrn.br

tendency for body size to increase over evolutionary time, Bergmann's rule[17], which describes the tendency for organisms to be larger in colder environments, and the Island Rule, which states the tendency for small species to become larger and large species smaller, on islands[18,19]. Depicting these rules provides us with insight into how environmental and ecological changes have shaped current biodiversity throughout evolution and helps us predict how species can adapt (or not) to the rapid environmental changes taking place today.

Few studies have yet addressed the evolutionary dynamics of body size in Siluriformes, so in this work we aimed to describe the evolutionary dynamics of body size in this group based on mitogenome data. To aid the analysis, we sequenced and assembled the mitogenome of *Brachyplatystoma filamentosum*, popularly known as Piraíba or Filhote, which is a commercially important species of catfish member of the Pimelodidae family and native to the Amazon basin[3]. *B. filamentosum* is the second largest freshwater fish in the Amazon region, second only to the Pirarucu (*Arapaima gigas*). Adult *B. filamentosum* specimens can weigh up to 150 kilograms and measure about 2 meters. The name Piraíba is commonly used for specimens larger than 1.6 m (about 50 kg), while Filhote is used for smaller ones[20]. There is limited information available in the literature on the biology of *B. filamentosum*, but evidence suggests that its natural stocks are being overexploited due to commercial fishing in the Amazon basin[20]. This largely impacts species conservation, as the minimum population doubling time of Piraíba is estimated to be over 14 years[3]. Studies involving sequencing, such as this, provide insights into the genetic diversity, phylogeography, and evolutionary scenario of the species, aiding the conservation and sustainable management of Piraíba.

Results

Mitogenomic structure and organization of Piraíba

The genomic data of *B. filamentosum* were generated from two adult specimens. The sequencing data of one sample were obtained with the PacBio platform and of the other sample, with the Illumina platform. Despite the differences in sequencing technologies, the assemblies were highly concordant, with the Illumina assembly measuring 16,566 bp and the PacBio assembly measuring 16,564 bp. The Illumina assembly exhibited a higher mean coverage (2,848.33x) compared to PacBio (490.27x), reflecting the larger number of reads (320,974 Illumina reads vs. 4,052 PacBio reads). This resulted in greater depth and more uniform coverage, with a minimum coverage of 1,320x and a maximum of 4,171x. Conversely, the PacBio assembly benefited from longer read lengths (average 3.259.02 bp for PacBio vs. 148.87 bp for Illumina), which facilitated resolution of repetitive regions and structural variants. Quality metrics also reflected the inherent differences in technology: Illumina reads had an average base quality of 32.68 and a mapping quality of 59.93, while PacBio reads had no base quality scores due to the nature of long-read sequencing but maintained a high mapping quality of 57.83. The BLAST alignment between the two assemblies showed a 99.67% identity over the entire length, with minimal gaps (2 out of 16,566 bp), confirming the high concordance and validating the accuracy of the assemblies. Discrepancies observed were minor and mainly located in homopolymeric regions, where PacBio reads tend to have a higher error rate. These were addressed by cross-validating with Illumina data.

The final consensus sequence of the complete circular mitogenome of Piraíba measured 16,566 bp in size and 42,2% in GC content. The mitogenome is composed of 13 protein-coding genes (PCGs), 22 tRNAs, and 2 rRNAs, of which 28 are accommodated in the H-strand (Heavy strand) (12 PCGs, 2 rRNAs, and 14 tRNAs), while *ND6* and 8 tRNAs (tRNA-E, tRNA-P, tRNA-Q, tRNA-A, tRNA-N, tRNA-C, tRNA-Y, and tRNA-S2) were positioned on the L-strand (Light strand) (Table 1, Fig. 1). The displacement loop (D-loop) was found between tRNA-F and tRNA-P and was 911 bp in length. The overall AT-skew and GC-skew were 0.128 and − 0.305, respectively. The start codons of all PCGs were ATG except for *COI*, which was GTG. Complete stop codon was found in 6 PCGs, of which 5 were TAA and one was TAG. The other 7 PCGs showed incomplete stop codons, in which 6 of them missed two nucleotides (T--) and one missed one nucleotide (TA-). The size of the tRNAs ranged from 67 and 75 base pairs. All 22 tRNAs showed the canonical cloverleaf structure except for tRNA-Ser (S1, anticodon: GCT), which did not show the dihydrouridine (D) arm (Fig. 2).

Time-calibrated phylogenetic tree and body size evolution in Siluriformes

The time-calibrated maximum likelihood (ML) tree generated from the mitogenome data (Fig. 3, Supplementary Figure 1, Supplementary Figure 2) estimated the origin of the order Siluriformes to be ∼ 118.4 Ma (CI 95% 122.6–114.3). In the basal portion of the Siluriformes clade, the clades encompassing the samples of the group Loricarioidei (genus *Corydoras, Hypostomus, Ancistrus, Pterygoplichthys*, and *Sturisomatichthys*) were the firsts to diversify, followed by the diversification of the clades encompassing the Diplomystoidei and Siluroidei suborders (∼ 98.5 Ma). The ML tree evidenced paraphyly of the suborder Loricarioidei. However, the tree topology test did not find a statistical difference between the likelihood of the ML tree and the tree supporting the monophyly of Loricarioidei. The origin of the Siluroidei suborder was estimated in 94.1 Ma (CI 95% 97.5–90.8) and right after its diversification, we observed the occurrence of short internal branches with low statistical support, characterizing a rapid expansion of the group. Nine clades presented high statistical support (> 95%) after the expansion event in Siluroidei: (1) the clade encompassing the species *Rita rita* (Ritidae) and *Plostosus lineatus* (Plotosidae), (2) Claroidea (Clariidae, and Heteropneustidae), (3) "Big Asia" (families Sisoridae, Amblycipitidae, Bagridae, and Ailiidae), (4) "Big Africa" (Amphiliidae, Auchenoglanididae, Claroteidae, Schilibidae, Malapteruridae and Mochokidae), (5) Ictaluroidea (Ictaluridae and Cranoglanididae) + Pangasiidae, (6) Pimelodoidea (Pimelodidae and Pseudopimelodidae), (7) Aspredinidae+Doradoidea (Doradidae and Auchenipteridae), (8) Arioidea (Ariidae), and (9) the unresolved family Siluridae. Considerable statistical support (88) was also found in the clade comprising Arioidea, Ictaluroidea, and Pangasiidae. Pimelodidae, the family to which the Piraíba belongs, is the sister group to the Pseudopimelodidae family, with an estimated origin at ∼ 46.3 Ma (CI 95% 48.6–44.0). The Piraíba sample is positioned as the sister group to the clade encompassing the samples of the genus

Genes	Start	Stop	Strand	Size (bp)	AntiCodon	Start Codon	Stop Codon
tRNA-Phe (F)	1	68	H	68	GAA		
12S rRNA	69	1028	H	960			
tRNA-Val (V)	1029	1100	H	72	TAC		
16S rRNA	1101	2778	H	1678			
tRNA-Leu (L2)	2779	2853	H	75	TAA		
ND1	2855	3826	H	972		ATG	TAA
tRNA-Ile (I)	3828	3899	H	72	GAT		
tRNA-Gln (Q)	3899	3969	L	71	TTG		
tRNA-Met (M)	3969	4038	H	70	CAT		
ND2	4039	5083	H	1045		ATG	T--
tRNA-Trp (W)	5084	5154	H	71	TCA		
tRNA-Ala (A)	5171	5239	L	69	TGC		
tRNA-Asn (N)	5241	5313	L	72	GTT		
tRNA-Cys (C)	5345	5411	L	67	GCA		
tRNA-Tyr (Y)	5413	5482	L	70	GTA		
COI	5484	7034	H	1551		GTG	TAA
tRNA-Ser (S2)	7035	7105	L	71	TGA		
tRNA-Asp (D)	7110	7182	H	73	GTC		
COII	7197	7887	H	691		ATG	T--
tRNA-Lys (K)	7888	7961	H	74	TTT		
ATP8	7963	8130	H	168		ATG	TAA
ATP6	8121	8803	H	683		ATG	TA-
COIII	8804	9587	H	784		ATG	T--
tRNA-Gly (G)	9588	9660	H	73	TCC		
ND3	9661	10009	H	349		ATG	T--
tRNA-Arg (R)	10010	10079	H	70	TCG		
ND4L	10080	10376	H	297		ATG	TAA
ND4	10370	11750	H	1381		ATG	T--
tRNA-His (H)	11751	11820	H	70	GTG		
tRNA-Ser (S1)	11821	11887	H	67	GCT		
tRNA-Leu (L1)	11895	11967	H	73	TAG		
ND5	11968	13794	H	1827		ATG	TAA
ND6	13791	14306	L	516		ATG	TAG
tRNA-Glu (E)	14307	14375	L	69	TTC		
Cytb	14377	15514	H	1138		ATG	T--
tRNA-Thr (T)	15515	15586	H	72	TGT		
tRNA-Pro (P)	15585	15654	L	70	TGG		
D-loop	15655	16565	H	911			

Table 1. Gene organization of *B. filamentosum* mitogenome.

Pseudoplatystoma and *Sorubim*. Considering the samples in the tree, their last divergence occurred at $\sim$ 40.8 Ma (CI 95% 43.1–38.6).

The body size of the Siluriformes species sampled in the tree shows a high degree of variation (Supplementary Table 1). In general, great variation in the body size can be found in all major groups of Siluriformes, except for the Loricarioidei, Diplomystoidei, and "Big Asia" groups, in which few samples reach 1 m in length. An extreme case is found within the Siluridae family, in which we can find specimens that can reach up to 4 m in length (*Silurus soldatovi*) and a sample no more than 10 cm long (*Kryptopterus vitreolus*). A similar scenario can be seen in the Pimelodidae family, where we could find the *B. filamentosum* specimen, which can reach 3.6 m, and the *Pimelodus pictus*, which reaches around 10 cm.

The evolutionary dynamics of log-transformed body size in the Siluriformes clade found 16 and 11 branches with significant positive and negative directional changes ($\beta \neq 1$), respectively, and 4 internal nodes with evolvability change (υ) above 1 (Fig. 3, Supplementary Table 2). In all major clades of Siluriformes, except for the "Big Africa" group, there was at least one branch with significant directional changes, either positive or negative, indicating the occurrence of abrupt changes in the body size. Most of the directional changes depicted occurred at the terminal branches, but we could depict positive directional changes at the basal portion of some Siluriformes clades, such as Pimelodidae, Siluridae, and the clade comprising Pangasiidae and Ictaluroidea. In the "Big Asia" group, we found two clades that showed significant changes in body size: (1) the clade involving the genus *Glyptothorax* (Sisoridae) and (2) the clade involving samples from the Bagridae (*Pseudobagrus*,

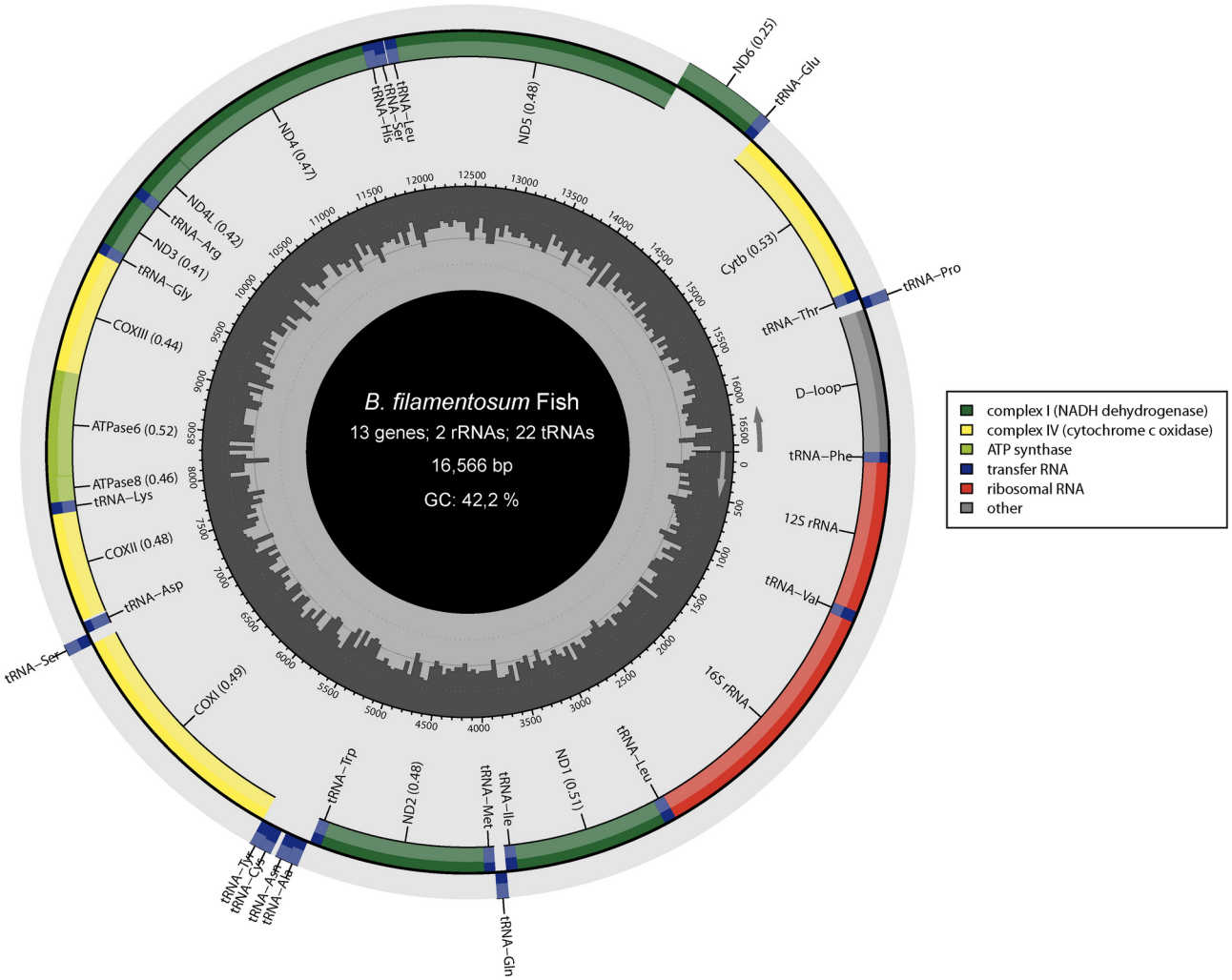

Figure 1. Circular map of the mitochondrial genome of *B. filamentosum*. Genes inside the circle are positioned in the H-strand, whereas those outside are positioned in the L-strand. Figure generated in the MitoAnnotator online server[68].

Pelteobagrus, *Tachysurus*, *Leiocassis*). In these clades, the analysis shows that the change in body size occurred with an increase in evolvability followed by the directional changes. The greatest rate of increase in growth in the Siluriform group was found at the branch leading up to the sample of *Silurus soldatovi*, which has grown 7.45 times its size over its branch (27.4 Ma). Other branches that had a considerable increase were those leading to the clade [*Clarias gariepinus* and *Clarias* sp.] (5.71x, over 38.5 Ma), *B. filamentosum* (5.65x, over 40.8 Ma), Pangasiidae (5.58x, over 26.3 Ma) and [*Ameiurus*, *Ictalurus* and *Pylodictis*] (4.89x, over 3.94 Ma). The highest rate of body size reduction in the Siluriformes group was found in the branch leading to the sample of *Noturus taylori*, which reduced its size 8.73 times over its branch (55.6 Ma) (Supplementary Table 2). We also run the model that includes a global directional trend parameter (βg) to assess evidence of general trends toward larger or smaller body size. The parameter βg was estimated to be close to zero, with a mean value of 0.00061 and a 95% HPD (highest posterior density) interval of − 0.0165 and 0.0157. This indicates no evidence of a global directional trend toward a larger or smaller body size along the tree.

Discussion

The mitogenome of Piraíba presented in this work represents the first sequenced in the genus *Brachyplatystoma*, and the 10th sequenced in the family Pimelodidae. The assembled mitogenome showed similar characteristics to the mitogenome of other species from the Pimelodoidea group (Pimelodidae and Pseudopimelodidae families) described so far, such as the mitogenome length (16,566 bp), percentage of GC content (42.21%), and the D-loop size (911 bp) (Table 2). The start and stop codons found among the PCGs of the Piraíba mitogenome, even the incomplete stop codons, were those commonly found in the fish mitogenomes, except for the *COIII*, which showed a stop codon (T--) that occurs in 10% of fish mitogenomes[21]. The genes in the mitogenome of *B. filamentosum* were also in complete synteny with the genes in the mitogenomes of other related species (Fig. 4). All these support the consistency of the mitogenome assembled in this work.

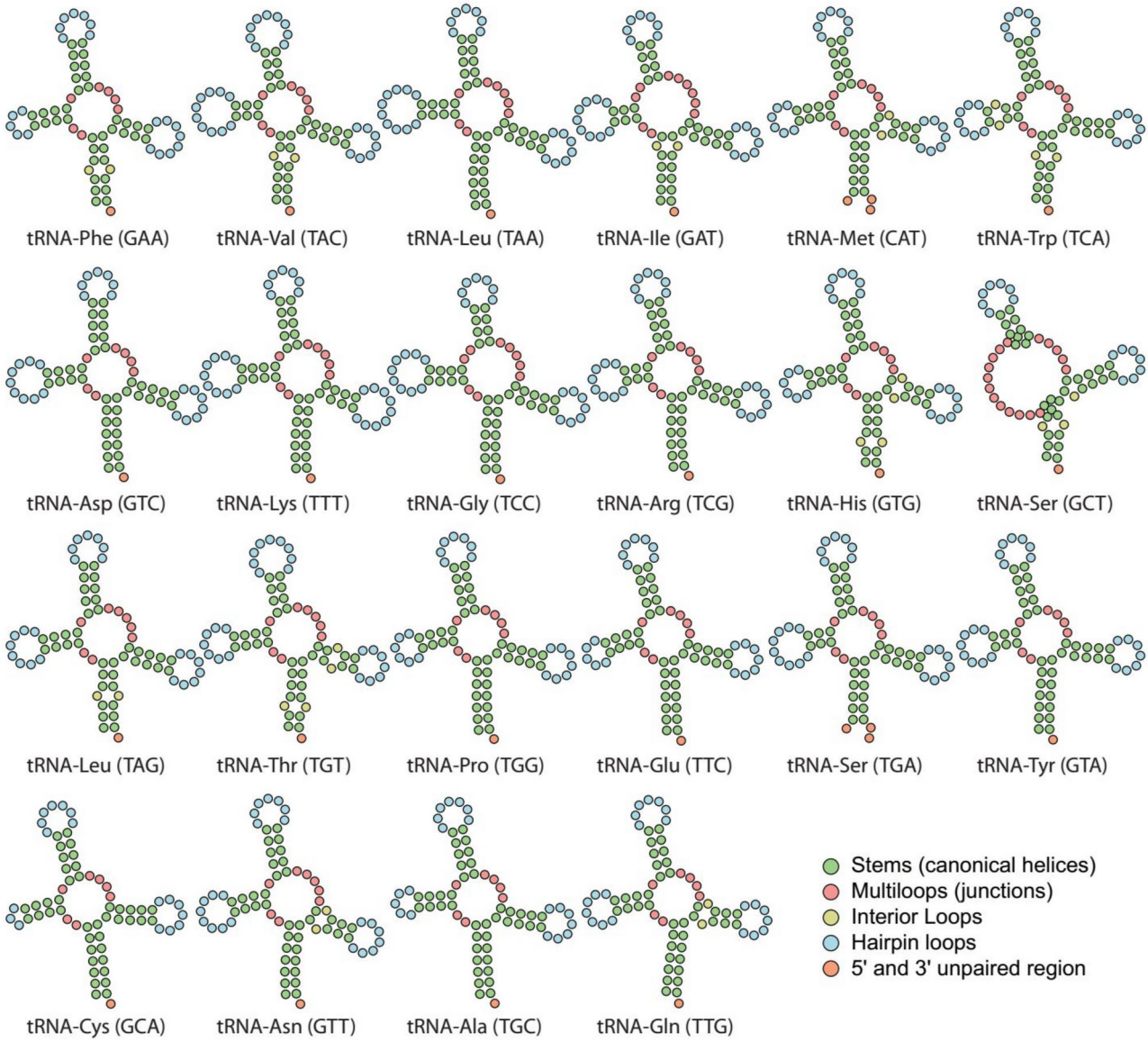

Figure 2. Putative secondary structure of 22 tRNA identified in *B. filamentosum* mitogenome. tRNA are shown in order of occurrence in the mitogenome starting from tRNA-Phe. Anticodons are in parentheses after the name of each tRNA.

As a commercially important species with signs of overexploitation[20], understanding the population structure and distribution of Piraíba is essential to guide conservation efforts. Next-generation sequencing-based methods have proven effective in monitoring biodiversity by assessing the environmental DNA[22,23]. Mitochondrial DNA is particularly favoured, as it is up to 1000 times more abundant than nuclear DNA in the environment[24]. Therefore, several studies have been carried out to provide reference mitogenomes from aquatic biodiversity[25,26]. In this sense, the wealth of mitogenomic data from Piraíba obtained in this work is a valuable resource, as it will allow the use of sequencing approaches to effectively assess its distribution and the possible impacts of its exploitation. It is noteworthy to mention the need for a larger effort in generating genomic resources in this group since the total number of mitogenomes from the Pimelodidae family sequenced so far corresponds to less than 10% of the current species diversity of the family, which totalizes 117 species described so far distributed in 32 genera[27].

Evolutionary history of Siluriformes

The phylogenetic analysis of the present study covered 137 species of Siluriformes (28 families), which doubled the number of samples used in the last work (62 samples, 21 families) that focused on this group and used mitogenome data[28]. The topology of the tree generated in this work largely corroborates with the inference made by Kappas et al.[28], with the most of interfamilar groups established by Sullivan et al.[29] being monophyletic groups with high statistical support. The tree generated in this study reveals the Loricarioidei group as the first group to

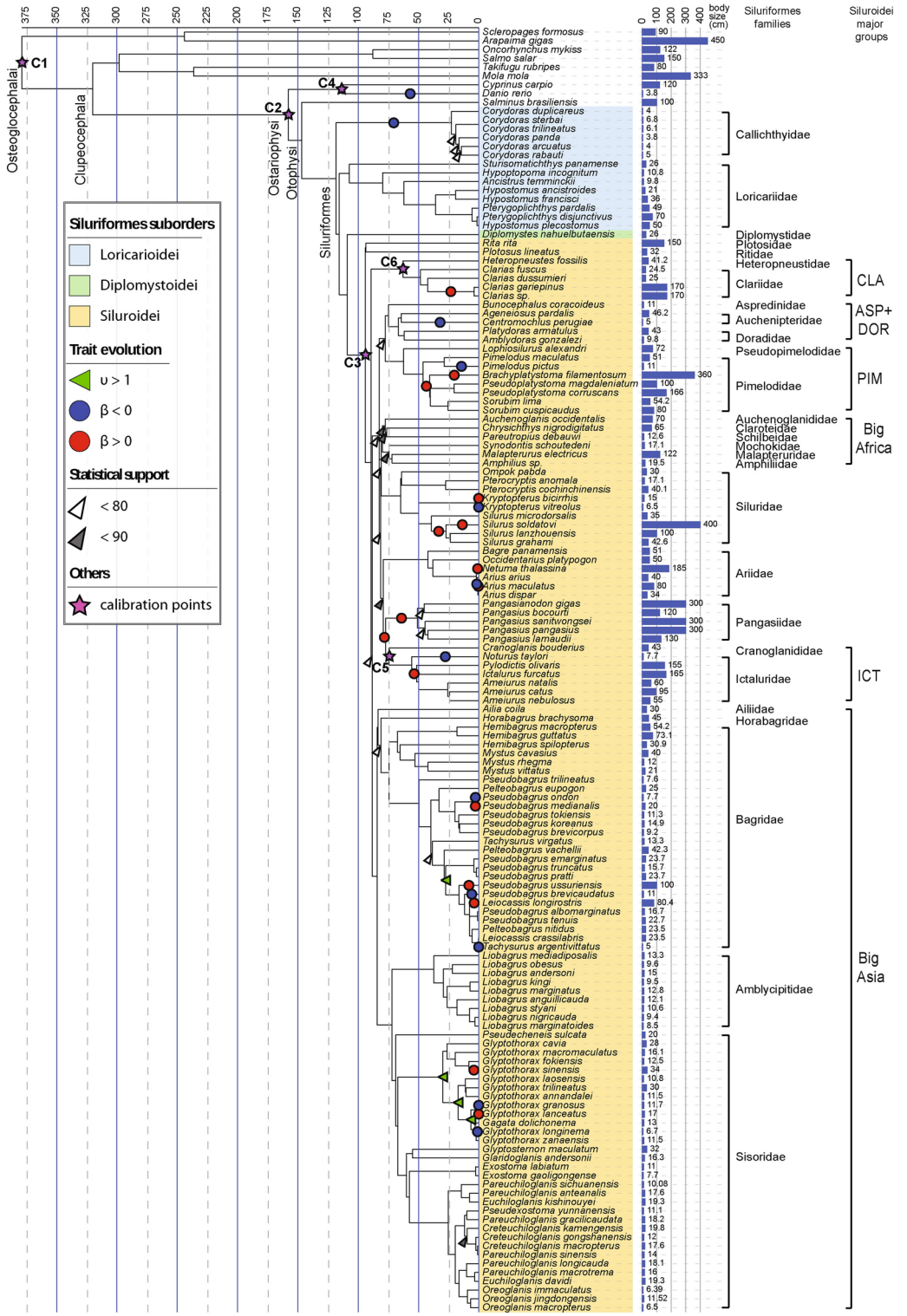

Figure 3. Time-calibrated maximum likelihood of Siluriformes order. Calibration points (C1-C6) are indicated in the tree with purple stars. Nodes with bootstrap statistical support below 80 and between 80 and 90 are indicated with white and gray arrowheads, respectively. Branches with significant positive and negative directional changes (β) are indicated with blue and red circles, respectively. Nodes with evolvability change (υ) above 1 are indicated with green left-pointing triangles. The bar chart represents the maximum body size (cm) of the samples in the tree. Legend: CLA: Claroidea, ASP+DOR: Aspredinidae+Doradoidea, PIM: Pimelodoidea, ICT: Ictaluroidea.

Family	Species	NCBI accession	Length (bp)	GC content (%)	D-loop size (bp)
Pimelodidae	*Brachyplatystoma filamentosum*	PQ380008.1	16,566	42.21	911
	Pimelodus maculatus	NC_032695	16,561	43.7	915
	Pimelodus pictus	NC_015797	16,575	42.57	923
	Pimelodus yuma	NC_061908	16,560	43.44	913
	Pseudoplatystoma corruscans	NC_026846	16,123	43.69	912
	Pseudoplatystoma magdaleniatum	NC_026526	16,568	44.19	912
	Pseudoplatystoma reticulatum	NC_033859	16,576	43.92	922
	Sorubim cuspicaudus	NC_026211	16,544	42.21	909
	Sorubim lima	NC_060300	16,539	43.0	897
	Steindachneridion melanodermatum	NC_065247	16,527	41.07	882
Pseudopimelodidae	*Lophiosilurus alexandri*	NC_026845	16,445	42.82	779
	Pseudopimelodus schultzi	NC_066072	16,455	41.9	805

Table 2. Characteristics of mitogenomes of species from the Pimelodoidea group sequenced so far.

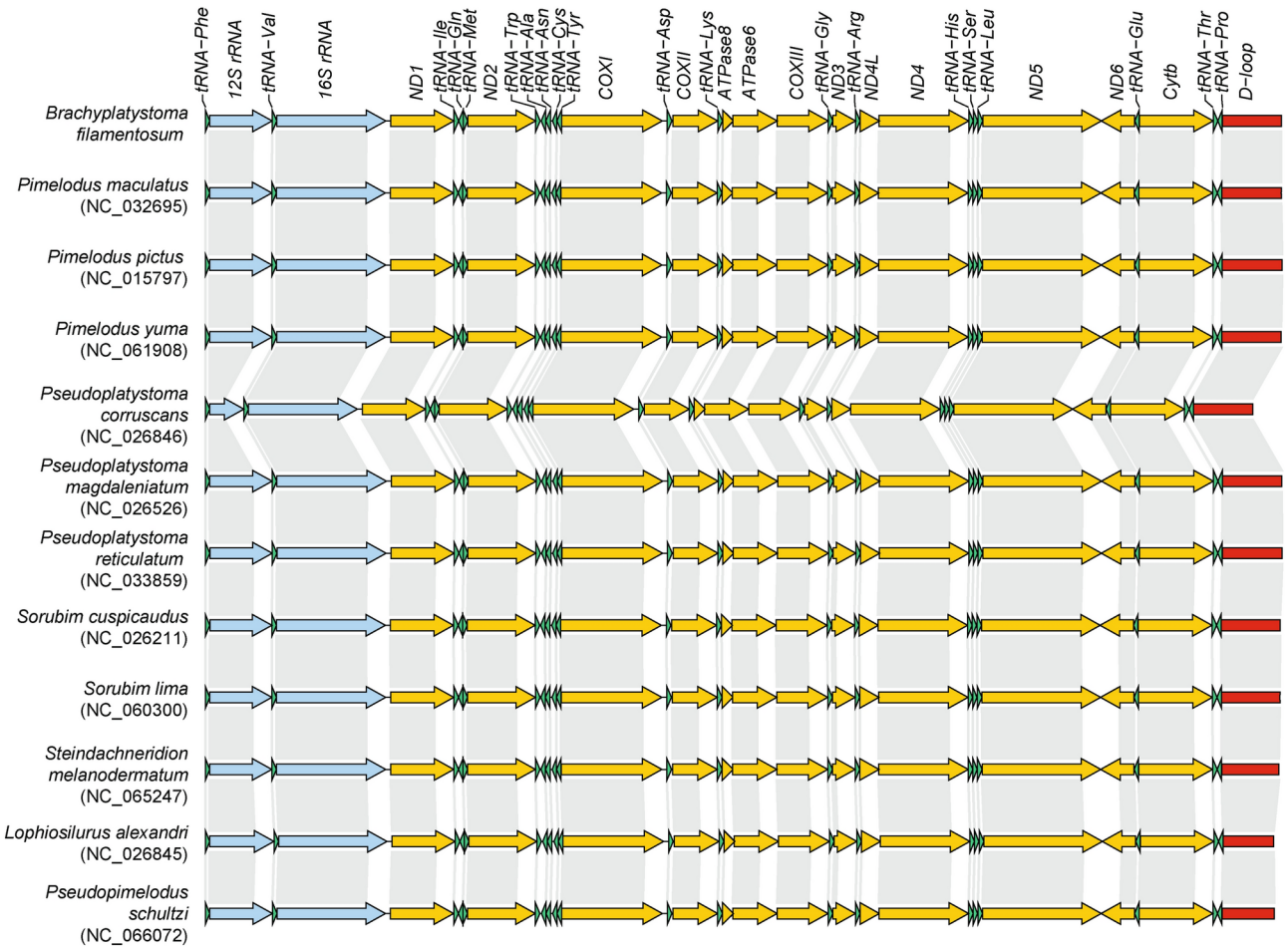

Figure 4. Synteny analysis among genes in the mitogenomes of *B. filamentosum* and of other species from group Pimelodoidea (Pimelodidae + Pseudopimelodidae). Links evidence genes/region with the same annotation. Legend of gene/region colors: blue: rRNA; green: tRNA, yellow: Protein coding sequence, red: D-loop.

diversify, followed by the diversification of Diplomystoidei and Siluroidei, as verified in other studies[28,29]. As the loricariids and diplostomids are distributed in the Neotropics region, the phylogenetic analysis also corroborates the "Out-of-South-America" hypothesis[29], indicating that the Neotropics region is the center of origin of the Siluriformes.

The tree also showed the condition of paraphyly in the Loricarioidei group, with the first diversification of the clade involving the genus *Corydoras* (Callichthyidae) and subsequent diversification of the members of the Loricariidae family. The paraphyly in Loricarioidei has been verified in other studies[28,30]. However, the phylogenetic studies with the *rag1* and *rag2* genes involving representatives of the six families of Loricariodei indicated to be monophyletic with a high support value[29]. The samples of loricarioids used in this study represent only two out of six families, so the paraphyly condition found in this group could be attributed to the low taxonomic sampling, which can reduce the resolution and accuracy of the phylogenetic inference[31]. This could also be verified by a tree topology test, which did not find statistical differences between the likelihood of the alternative tree (monophyly of Loricarioidei) and the likelihood of the ML tree. The inclusion of mitogenome data from the remaining families (Astroblepidae, Nematogenyidae, Scoloplacidae and Trichomycteridae) in the analysis should help to define the correct status of the Loricarioidei group. Another procedure that could lead to more reliable conclusions about the evolution of Siluriformes is to increase the total length of nucleotides analysed for each sample by including nuclear gene sequences[32].

In the suborder Siluroidei, the basal portion of its clade has short branches and internal nodes with low support values, characterizing a rapid expansion of the group. The large interfamilial groups traditionally recognized[29] formed monophyletic groups with a high support value in the maximum likelihood tree obtained in this study. Additionally, we observed two clades with high support: one includes the Ictaluroidea group and the Pangasiidae family (bootstrap value: 100) and the second includes the previous clade and the Ariidae family (bootstrap value: 88). These corroborate with a recent study[33] focusing on the Pangasiidae mitogenome, which found that Austroglanididae (not sampled in this study) forms the sister group of Pangasiidae and that they formed a clade with a considerable bootstrap value with the Ictaluroidea and Ariidae groups. The tree also shows a clade formed by samples of *Rita rita* (Ritidae) and *Plotosus lineatus* (Plotosidae). Despite their high support value, the grouping of these samples could be due to the long branch attraction and could not represent a reliable topology. As suggested for Loricarioidei group, the inclusion of more samples from members of these families and from families not sampled in this study and which remain unresolved, such as Cetopsidae and Chacidae, or increasing the total length of nucleotide analysed may help to find other higher level relationships between the families of Siluroidei group.

The diversification times in this work were inferred using the maximum likelihood approach of the RelTime method[34], which was demonstrated to outperform other methods[35–37], especially when dealing with trees with relaxed molecular clocks. We attempted to perform the Bayesian approach implemented by the BEAST program[38], which is largely used for divergence time inference. However, the independent runs failed to converge, probably due to the low phylogenetic resolution in the basal portion of the Siluroidei clade. The evolution of the Siluriformes order has been extensively studied, either by morphological (see (Diogo and Peng 2010[39])) or molecular data[28–30], but there are still debates concerning its origin. Estimates on the origin of Siluriformes found in other works have a wide margin ranging from 180 Ma to 88 Ma (Table 3). They can be subdivided into those arguing the origin in the Early or Late Cretaceous. The Early Cretaceous origin of this group, anticipating the complete separation of the supercontinent of Gondwana and Laurasia (~140 Ma), could explain the wide paleogeographic distribution of the order. However, this inference has a low reconciliation with the fossil data, since the oldest fossil records of the group are from the Late Cretaceous. The time-calibrated tree inferred in this work suggests that the origin of Siluriformes (~114 Ma) was in the Late Cretaceous, meanwhile, the origin of Siluroidei post-dated the complete separation of South America and Africa (100 Ma). This estimate is close to the date of the oldest fossil described for the crown group Siluriformes (83.5-88.6 Ma), demonstrating a good reconciliation between the molecular and fossil data. In the meantime, it is important to note that our estimate on the origin of Siluriformes is largely constrained by the maximum age of the calibration time on the origin of Ostariophysi (158.3 Ma). Therefore, any update on the maximum age of this node will largely affect the inference of Siluriformes' origin.

Evolutionary dynamics of body size in Siluriformes

Fish are important models that allowed us to understand the influence of various biotic and abiotic factors on body size. Several effects resulting from anthropogenic actions on the waters, such as acidification, increase in temperature, pollution, overfishing, and habitat destruction, could be observed to promote changes in the body size of the fish population[4]. The Siluriformes is an interesting group for studying the evolutionary dynamics of

Work	Origin of Siluriformes	Origin of siluroidei	Data
Santini et al.[86]	88 Ma (77-98)		*rag1*
Chen et al.[87]	97 Ma (86-109)	78.7 Ma (72-86)	*rag1*, *rho*, *egr1*, *egr2b*, and *egr3*
Near et al.[88]	106.1 Ma (89.9-123.0)		*glyt*, *myh6*, *plagl2*, *Ptr*, *rag1*, *sh3px3*, *sreb2*, *tbr1*, and *zic1*
This work	118.4 Ma	94.1 Ma	Mitogenome
Saitoh et al.[89]	125 Ma (104-148)		Mitogenome
Kappas et al.[28]	133.11 Ma	97.04 Ma	Mitogenome
Peng et al.[90]	173 Ma		Mitogenome
Nakatani et al.[91]	180 Ma (162-198)		Mitogenome

Table 3. Inference on Siluriformes and Siluroidei origin among studies.

body size since it is a broad group with a wide range of sizes. However, there are still few studies addressing this topic in this group[40,41].

The temperature, in particular, is an important factor that influences the fish's body size since they are ectothermic organisms and therefore more sensitive to its change[42]. The rise in the water temperature diminishes aerobic capacity, driving the selection towards smaller fishes[42,43]. The negative correlation between temperature and body size is described by Bergmann's rule and several studies have found support for this rule in fishes[44,45]. A correlation analysis between the ocean temperature and marine fish body size throughout the geological era verified that the gradual decrease in sea surface temperature is accompanied by a gradual increase in the mean fish body size during the period encompassing the late Cretaceous (~100 Ma) to the present day[46]. Global trend for body size reduction in response to global warming was also found in specific taxonomic groups of fish[42,43]. In our study, the estimation of the global directional trend parameter (βg) was near zero, indicating, at first, no evidence for a global trend toward either a larger or smaller body size along the Siluriformes evolution. This may be attributed to the variety of habitats and niches occupied by the sampled Siluriformes species. It is worth noting that as the period under study is characterised by several major ecological events, such as climate change, mass extinctions and ecological transitions, it is possible that the living sampled members are not be representative of the body size diversity that existed in the ancestral populations. As this could lead to misinterpretation of the evolution of a trait[47], the inclusion of morphological data from the fossil record is necessary to detect possible macroevolutionary patterns of body size change in response to the environmental pressures[48]. Fortunately, there are several fossil records in the order Siluriformes, which will allow future studies to better understand the evolutionary dynamics of body size in this group.

Another remarkable characteristic of the Siluriformes group is the capacity of several representatives to produce venom[49]. The venom glands in Siluriformes are located near the dorsal and pectoral fins with a bony structure that helps in the venom delivery against predators[50]. This characteristic might have appeared in the early time of the evolutionary history of Siluriformes[49], suggesting that early ancestors of Siluriformes occupied a lower trophic level. Along the evolution, some lineages have suffered loss of the venom gland, or a decrease in the morphological complexity of the bone structure as a result of the relaxation of the selective pressure for its maintenance[49,51]. Ontogenetic loss of the venom gland is also observed in some species when their body size reaches a certain length that protects them from their predators[52], which should be driven to reduce the energy cost of maintaining venom production. All this evidence demonstrates an intricate relationship between body size, venom production, and predators, which should have operated throughout the evolution of the Siluriformes. In this sense, the prey vulnerability model could be one reasonable explanation for the changes toward smaller or larger sizes depicted by the fabric model in some recent lineages of the Siluriformes group. The prey vulnerability is modeled by a dome-shaped curve, suggesting that the risk of predation of smaller and larger individuals is lower than that of middle-sized ones[53,54].

We also highlight the evidence of abrupt changes toward larger size in the early evolution of the families Pimelodidae, Siluridae, Pangasiidae, and Ictaluridae. The evolutionary time of this change occurred near after the rapid expansion of the Siluriformes group and close to the mass extinction event that occurred during Cretaceous-Paleogene (~66 Ma) and Paleocene-Eocene Thermal Maximum (~55.6 Ma). The first is known to have been caused by an asteroid collision on Earth[55,56], while the second is characterized by the rise of the average global temperature in 5–8 °C and massive input of carbon into the ocean and atmosphere[57]. The biodiversity loss caused by these events drastically changed the food web dynamics[58,59]. For the catfish survivors, the event may have reduced their predators, favoring the shift of some Siluriformes lineages to the predator condition. It is interesting to note that the diversification of the group before the mass extinction event may have been crucial in the survival of the group, as suggested in terrestrial animals[60].

Body size also has a profound impact on speciation rates[61]. In fishes of South America freshwaters, it was noted a rapid species expansion in clades comprised of small-bodied fishes[61]. A similar observation was also made in a phylodynamics analysis in the family Ictaluridae, in which small body size was a significant predictor of species richness[40]. It was suggested that a larger body size confers a high mobility capacity, allowing gene flow maintenance among its subpopulation. On the other hand, the low mobility in small-bodied fishes isolates their subpopulations and accelerates the speciation process[40].

The evolutionary analysis performed in this work also identified some clades that could be addressed to understand the genetic basis underlying the diversity of the body size in Siluriformes. Families such as Pimelodidae, Siluridae, Ictaluridae, and Ariidae, are interesting targets due to the presence of clades that underwent abrupt change either for larger or smaller body size. One study addressing this issue used the transcriptomic approach and identified 20 candidate genes that could be associated with the body size in representatives of the family Sisoridae[41]. Studies involving the genomic approach in other Siluriformes families are of great interest to support these findings.

Methods

Samples, DNA extraction and sequencing

Two fresh adult specimens of *Brachyplatystoma filamentosum* (NCBI Taxonomy ID: 642922, FishBase ID: 6420) were collected at the Ver-o-Peso market in Belém, Pará, Brazil. The specimens, already deceased, were transported on ice to the Laboratory of Ecology and Conservation at the Federal University of Pará, where they were stored at − 20 °C. Genomic DNA was extracted from the pectoral fin tissues using the phenol-chloroform method[62]. The concentration and quality of the extracted DNA were evaluated using a NanoDrop 1000 spectrophotometer (Thermo Fisher Scientific, Wilmington, DE, USA) to confirm its suitability for subsequent analyses.

The genomic library of one sample was prepared using the SMRTbell Template Kit 1.0 (PN: 100-259-100 Pacific Biosystems, Menlo Park, CA, USA) following the manufacturer's recommended protocols. The sequencing process was conducted on a PacBio Sequel I system (Pacific Biosystems), utilizing a SMRT Cell 1M v3 (PN: 101-

Node	Taxonomic group	Fossil species	Age	References
C1	crown-group of Actinopterygii	†*Moythomasia durgaringa*	422.4–378.19 Ma (Uniform distribution)	Benton et al.[92]
C2	tMRCA of Ostariophysi	†*Rubiesichthys gregalis*	158.3–126.3 Ma (Uniform distribution)	Benton et al.[92]
C3	tMRCA of the crown-group Siluroidei	Siluroid fossils from the Campanian stage in South America	Min. time: 70.6 Ma	Gayet and Otero[93]
C4	tMRCA of the clade (*Danio*, *Cyprinus*)	†*Parabarbus* (Cyprinidae)	Min. time: 49 Ma	Sytchevskaya[94]
C5	Total group Ictaluridae	†*Astephus sp.*	Min. time: 63 Ma	Divay and Murray[95]
C6	tMRCA of the clade (*Clarias*, *Heteropneustes*)	First appearance of the African Clariidae in the Lower Eocene	Min. time: 34 Ma	M. Gayet and Meunier[96]

Table 4. Fossil data used for phylogenetic time-calibration.

531-000) and a Sequel Sequencing Kit 3.0 (4 Reaction Plate) (PN: 101-597-900). For the second sample, its genomic library was prepared using the Illumina DNA prep kit (Illumina, San Diego, CA, USA) according to the manufacturer's instructions with a short insert size of 500 bp. The library was then sequenced on a NextSeq 550 Illumina platform using a paired-end High Output kit v2 (300 cycles, Illumina, San Diego, CA, USA).

Mitogenome assembly, and genomic characterization

The mitochondrial genome assembly procedures were conducted separately for the Illumina and PacBio sequencing. The assembly of Illumina reads, performed with NOVOPlasty v.4.3[63], was circularized and confirmed by Unicycler v.0.5.0[64]. Similarly, the assembly of PacBio reads, performed with Organelle PBA v.1.0.8[65], was also circularized and confirmed by Unicycler. The use of two assemblers was adopted as a strategy to validate the mitochondrial genomic structure. The mtDNA generated by NOVOPlasty was used as a reference sequence to retrieve the mitochondrial reads necessary for subsequent assembly by Unicycler. BWA v.0.7.18[66] was used for mapping the Illumina reads, and pbmm2 v.1.13.1 (https://github.com/PacificBiosciences/pbmm2) was used for the PacBio reads, while bamTofastq implemented in BEDTools[67] was used for read conversion.

The annotation of the mitochondrial genome was performed using the web servers Mitos (http://mitos.bioinf.uni-leipzig.de) and MitoAnnotator (http://mitofish.aori.u-tokyo.ac.jp/annotation/input/), implemented in Mitofish[68], for mitochondrial DNA annotation[68,69]. The tRNA genes were analyzed with tRNAscan-SE 2.0[70], using the default settings for the vertebrate mitochondrial genetic code. Additionally, the prediction of the secondary structures of tRNAs was performed with tRNAscan-SE, and forna[71] was used to visualize these structures. The strand asymmetry was determined using the formula AT-skew = (A − T)/(A + T) and GC-skew = (G − C)/(G + C)[72].

Genome and body size data from public databases

The nucleotide sequences of coding regions, tRNA, and rRNA from the mitogenomes of other Siluriformes fishes were retrieved from the NCBI Genome database in March 2022. At that time, 154 complete or nearly complete Siluriformes mtDNA sequences were available, representing 28 out of 39 Siluriformes families. To ensure the quality and reliability of the phylogenetic and evolutionary analyses, six samples were excluded: three from hybrid species and three with missing mitochondrial genes. Given computational constraints, we conducted a preliminary phylogenetic analysis to select representative samples from each Siluriformes family while preserving taxonomic diversity. As a result, the dataset comprised 136 mtDNA samples from NCBI, plus the mtDNA of *B. filamentosum* sequenced in this study, representing 28 Siluriformes families. Additionally, nucleotide sequences from 10 non-Siluriformes mtDNA samples, representing the orders Characiformes, Cypriniformes, Ceratodontiformes, Tetraodontiformes, Salmoniformes, and Osteoglossiformes, were retrieved to serve as outgroups in the phylogenetic analysis (Supplementary Table 1).

The maximum body size registered for each fish sample used for the trait evolution analysis was retrieved from the FishBase database[27]. All retrieved values were log-transformed before applying them to any analysis performed in this work. It is important to note that FishBase provides the Standard Length of the body size for most samples. However, for some samples, only the Total Length is provided. Since the difference between the log-transformed values of Standard Length and Total Length is small, we used both measures interchangeably in this work.

Phylogenetic analyses and evolutionary dynamics of body size

To perform the evolutionary inference of the order Siluriformes, the nucleotide sequences of each mitogenome gene set (coding sequences, tRNA, and rRNA) were aligned using MUSCLE[73], and the resulting alignments were manually inspected using MEGA X[74]. For the alignment of protein-coding sequences, the nucleotide sequences were translated to amino acids using SeqKit[75], aligned with MUSCLE, and back-translated to nucleotides using PAL2NAL[76]. Then, a phylogenetic tree was inferred using the Maximum Likelihood approach with iqTree (v.2)[77]. For this, the alignment was partitioned by codon position, tRNA, and rRNA as suggested by[78]. The tree was rooted using the mitogenome of *Neoceratodus fosteri* as an outgroup. The molecular timing of species divergences was estimated with the RelTime[36] implemented in the software Mega X[74]. For this, six nodes (C1, C2, C3, C4, C5, and C6) were considered as time-calibrated points (Table 4).

To elucidate the evolutionary dynamics of body size in the order Siluriformes, we carried out the estimation of the β (directional change) and υ (evolvability change) parameters from the Fabric model[9]. These parameters were estimated using the BayesTraits program[79,80]. For this analysis, we used as input the time-calibrated

maximum likelihood tree and the log-transformed data on the body size of the samples that were extracted from the FishBase database[27]. We carried out six independent runs, each with 30M iterations, and sampled every 1000 iterations. The results were checked for parameter convergence using the Tracer program[81] and then summarized by the FabricPostProcessor program[9]. Parameters were considered to have altered values ($\beta \neq 0$ and $\upsilon \neq 1$) when they were altered in at least five of the six independent runs. We also carried out an analysis that additionally estimates the global directional change parameter (βg) from the Fabric model to verify evidence of a global trend toward smaller or bigger body sizes along the tree.

Visualization tools

Visualization of the circular mtDNA genome was made by MitoAnnotator online server[68]. The scheme on the mtDNA gene organization in multiple samples was made using LinearDisplay[82]. Phylogenetic tree visualization, inspection, and annotation with taxonomic and morphological data were made using the software TaxOnTree[83] and FigTree[84]. The final tree was generated using iTol[85].

Data availability

The mitogenome sequence of *B. filamentosum* generated during the current study was deposited in the NCBI database under the accession number PQ380008.1 (https://www.ncbi.nlm.nih.gov/nuccore/PQ380008.1/).

Received: 24 November 2024; Accepted: 12 March 2025
Published online: 21 March 2025

References

1. Fricke, R., Eschmeyer, W. & Van der Laan, R. *Catalog of Fishes: Genera, Species, References*. California Academy of Sciences. http://researcharchive.calacademy.org/research/ichthyology/catalog/fishcatmain.asp (2018).
2. Nelson, J. S., Grande, T. C. & Wilson, M.V. *Fishes of the World* (Wiley, 2016).
3. Reis, R. E. *Check List of the Freshwater Fishes of South and Central America* (Edipucrs, 2003).
4. Ahti, P. A., Kuparinen, A. & Uusi-Heikkilä, S. Size does matter—The eco-evolutionary effects of changing body size in fish. *Environ. Rev.* **28**, 311–324. https://doi.org/10.1139/er-2019-0076 (2020).
5. Slater, G. J., Price, S. A., Santini, F. & Alfaro, M. E. Diversity versus disparity and the radiation of modern cetaceans. *Proc. R. Soc. B Biol. Sci.* **277**, 3097–3104. https://doi.org/10.1098/rspb.2010.0408 (2010).
6. Burin, G., Park, T., James, T. D., Slater, G. J. & Cooper, N. The dynamic adaptive landscape of cetacean body size. *Curr. Biol.* **33**, 1787-1794.e3. https://doi.org/10.1016/j.cub.2023.03.014 (2023).
7. Webster, A. J., Gittleman, J. L. & Purvis, A. The life history legacy of evolutionary body size change in carnivores. *J. Evol. Biol.* **17**, 396–407. https://doi.org/10.1046/j.1420-9101.2003.00664.x (2004).
8. Huang, X. et al. Genomic insights into body size evolution in Carnivora support Peto's paradox. *BMC Genomics* **22**, 429. https://doi.org/10.1186/s12864-021-07732-w (2021).
9. Pagel, M., O'Donovan, C. & Meade, A. General statistical model shows that macroevolutionary patterns and processes are consistent with Darwinian gradualism. *Nat. Commun.* **13**, 1113. https://doi.org/10.1038/s41467-022-28595-z (2022).
10. Boback, S. M. Body size evolution in snakes: Evidence from island populations. *Copeia* **2003**, 81–94. https://doi.org/10.1643/0045-8511(2003)003[0081:BSEISE]2.0.CO;2 (2003).
11. Slavenko, A. et al. Global patterns of body size evolution in squamate reptiles are not driven by climate. *Glob. Ecol. Biogeogr.* **28**, 471–483. https://doi.org/10.1111/geb.12868 (2019).
12. Wu, H., Gao, S., Xia, L. & Li, P. Evolutionary rates of body-size-related genes and ecological factors involved in driving body size evolution of squamates. *Front. Ecol. Evol.*. https://doi.org/10.3389/fevo.2022.1007409 (2022).
13. Farina, B. M., Godoy, P. L., Benson, R. B. J., Langer, M. C. & Ferreira, G. S. Turtle body size evolution is determined by lineage-specific specializations rather than global trends. *Ecol. Evol.* **13**, e10201. https://doi.org/10.1002/ece3.10201 (2023).
14. Chown, S. L. & Gaston, K. J. Body size variation in insects: A macroecological perspective. *Biol. Rev.* **85**, 139–169. https://doi.org/10.1111/j.1469-185X.2009.00097.x (2010).
15. Cope, E. D. *The Origin of the Fittest: Essays on Evolution* (D. Appleton, 1887).
16. Stanley, S. M. An explanation for Cope's rule. *Evolution* **27**, 1–26. https://doi.org/10.1111/j.1558-5646.1973.tb05912.x (1973).
17. Bergmann, C. About the relationships between heat conservation and body size of animals. *Goett. Stud.* **1**, 595–708 (1847).
18. Van, V. A new evolutionary law. *Evol. Theory* **1**, 1 (1973).
19. Lomolino, M. V. Body size of mammals on islands: The island rule reexamined. *Am. Nat.* **125**, 310–316. https://doi.org/10.1086/284343 (1985).
20. Petrere, M., Barthem, R. B., Córdoba, E. A. & Gómez, B. C. Review of the large catfish fisheries in the upper Amazon and the stock depletion of piraíba (*Brachyplatystoma filamentosumLichtenstein*). *Rev. Fish Biol. Fish.* **14**, 403–414. https://doi.org/10.1007/s11160-004-8362-7 (2004).
21. Satoh, T. P., Miya, M., Mabuchi, K. & Nishida, M. Structure and variation of the mitochondrial genome of fishes. *BMC Genomics* **17**, 719. https://doi.org/10.1186/s12864-016-3054-y (2016).
22. Carroll, E. L. et al. Genetic and genomic monitoring with minimally invasive sampling methods. *Evol. Appl.* **11**, 1094–1119 (2018).
23. Beng, K. C. & Corlett, R. T. Applications of environmental dna (edna) in ecology and conservation: Opportunities, challenges and prospects. *Biodivers. Conserv.* **29**, 2089–2121 (2020).
24. Johnson, R. N., Wilson-Wilde, L. & Linacre, A. Current and future directions of dna in wildlife forensic science. *Forensic Sci. Int. Genet.* **10**, 1–11 (2014).
25. Alvarenga, M. et al. Mitochondrial genome structure and composition in 70 fishes: A key resource for fisheries management in the South Atlantic. *BMC Genomics* **25**, 215 (2024).
26. Diver, T. A. et al. Increasing availability of reference mitochondrial genomes for imperiled fishes in western North America for environmental dna assay design and species monitoring. *Fronti. Conserv. Sci.* **5**, 1294358 (2024).
27. Froese, R. & Pauly, D. Fishbase. https://www.fishbase.org (2024). Version (06/2024). World Wide Web electronic publication. R. Froese and D. Pauly.
28. Kappas, I., Vittas, S., Pantzartzi, C. N., Drosopoulou, E. & Scouras, Z. G. A Time-calibrated mitogenome phylogeny of catfish (Teleostei: Siluriformes). *PLOS ONE* **11**, e0166988. https://doi.org/10.1371/journal.pone.0166988 (2016).
29. Sullivan, J. P., Lundberg, J. G. & Hardman, M. A phylogenetic analysis of the major groups of catfishes (Teleostei: Siluriformes) using rag1 and rag2 nuclear gene sequences. *Mol. Phylogenet. Evol.* **41**, 636–662. https://doi.org/10.1016/j.ympev.2006.05.044 (2006).

30. Hardman, M. The phylogenetic relationships among non-diplomystid catfishes as inferred from mitochondrial cytochrome b sequences: The search for the ictalurid sister taxon (Otophysi: Siluriformes). *Mol. Phylogenet. Evol.* **37**, 700–720. https://doi.org/10.1016/j.ympev.2005.04.029 (2005).
31. Zwickl, D. J. & Hillis, D. M. Increased taxon sampling greatly reduces phylogenetic error. *Syst. Biol.* **51**, 588–598 (2002).
32. Rosenberg, M. S. & Kumar, S. Taxon sampling, bioinformatics, and phylogenomics. *Syst. Biol.* **52**, 119 (2003).
33. Duong, T. Y. et al. Mitophylogeny of Pangasiid catfishes and its taxonomic implications for Pangasiidae and the suborder Siluroidei. *Zool. Stud.* **62**, e48. https://doi.org/10.6620/ZS.2023.62-48 (2023).
34. Tamura, K. et al. Estimating divergence times in large molecular phylogenies. *Proc. Natl. Acad. Sci. USA* **109**, 19333–19338. https://doi.org/10.1073/pnas.1213199109 (2012).
35. Mahony, S., Foley, N. M., Biju, S. & Teeling, E. C. Evolutionary history of the asian horned frogs (Megophryinae): Integrative approaches to timetree dating in the absence of a fossil record. *Mol. Biol. Evol.* **34**, 744–771. https://doi.org/10.1093/molbev/msw267 (2017).
36. Tamura, K., Tao, Q. & Kumar, S. Theoretical foundation of the RelTime method for estimating divergence times from variable evolutionary rates. *Mol. Biol. Evol.* **35**, 1770–1782. https://doi.org/10.1093/molbev/msy044 (2018).
37. Barba-Montoya, J., Tao, Q. & Kumar, S. Assessing rapid relaxed-clock methods for phylogenomic dating. *Genome Biol. Evol.* **13**, evab251. https://doi.org/10.1093/gbe/evab251 (2021).
38. Suchard, M. A. *et al.* Bayesian phylogenetic and phylodynamic data integration using BEAST 1.10. *Virus Evol.* **4**, vey016. https://doi.org/10.1093/ve/vey016 (2018).
39. Diogo, R. & Peng, Z. *State of the Art of Siluriform Higher-level Phylogeny* 465–515. https://doi.org/10.1201/b10194-13 (2010).
40. Hardman, M. & Hardman, L. M. The relative importance of body size and paleoclimatic change as explanatory variables influencing lineage diversification rate: An evolutionary analysis of bullhead catfishes (Siluriformes: Ictaluridae). *Syst. Biol.* **57**, 116–130. https://doi.org/10.1080/10635150801902193 (2008).
41. Jiang, W., Guo, Y., Yang, K., Shi, Q. & Yang, J. Insights into body size evolution: A comparative transcriptome study on three species of Asian Sisoridae catfish. *Int. J. Mol. Sci.* **20**, 944. https://doi.org/10.3390/ijms20040944 (2019).
42. Baudron, A. R., Needle, C. L., Rijnsdorp, A. D. & Tara Marshall, C. Warming temperatures and smaller body sizes: Synchronous changes in growth of North Sea fishes. *Glob. Change Biol.* **20**, 1023–1031. https://doi.org/10.1111/gcb.12514 (2014).
43. Daufresne, M., Lengfellner, K. & Sommer, U. Global warming benefits the small in aquatic ecosystems. *Proc. Natl. Acad. Sci.* **106**, 12788–12793. https://doi.org/10.1073/pnas.0902080106 (2009).
44. Knouft, J. H. Latitudinal variation in the shape of the species body size distribution: An analysis using freshwater fishes. *Oecologia* **139**, 408–417. https://doi.org/10.1007/s00442-004-1510-x (2004).
45. Rypel, A. L. The cold-water connection: Bergmann's rule in North American freshwater fishes. *Am. Nat.* **183**, 147–156. https://doi.org/10.1086/674094 (2014).
46. Troyer, E. M. et al. The impact of paleoclimatic changes on body size evolution in marine fishes. *Proc. Natl. Acad. Sci.* **119**, e2122486119. https://doi.org/10.1073/pnas.2122486119 (2022).
47. Hunt, G. & Slater, G. Integrating paleontological and phylogenetic approaches to macroevolution. *Annu. Rev. Ecol. Evol. Syst.* **47**, 189–213 (2016).
48. Quental, T. B. & Marshall, C. R. Diversity dynamics: Molecular phylogenies need the fossil record. *Trends Ecol. Evol.* **25**, 434–441. https://doi.org/10.1016/j.tree.2010.05.002 (2010).
49. Wright, J. J. Diversity, phylogenetic distribution, and origins of venomous catfishes. *BMC Evol. Biol.* **9**, 282. https://doi.org/10.1186/1471-2148-9-282 (2009).
50. Harris, R. J. & Jenner, R. A. Evolutionary ecology of fish venom: Adaptations and consequences of evolving a venom system. *Toxins* **11**, 60. https://doi.org/10.3390/toxins11020060 (2019).
51. Wright, J.J. Evolutionary history of venom glands in the Siluriformes. In Gopalakrishnakone, P. & Malhotra, A. (eds.) *Evolution of Venomous Animals and Their Toxins* 1–19. https://doi.org/10.1007/978-94-007-6727-0_9-1 (Springer, 2015).
52. Egge, J. J. D. & Simons, A. M. Evolution of venom delivery structures in madtom catfishes (Siluriformes: Ictaluridae). *Biol. J. Linn. Soc.* **102**, 115–129. https://doi.org/10.1111/j.1095-8312.2010.01578.x (2011).
53. Heins, D. C., Knoper, H. & Baker, J. A. Consumptive and non-consumptive effects of predation by introduced northern pike on life-history traits in threespine stickleback. *Evol. Ecol. Res.* **17**, 355–372 (2016).
54. Reznick, D., Butler, M. J. IV. & Rodd, H. Life-history evolution in guppies. vii. The comparative ecology of high-and low-predation environments. *Am. Nat.* **157**, 126–140 (2001).
55. Smit, J. & Hertogen, J. An extraterrestrial event at the Cretaceous–Tertiary boundary. *Nature* **285**, 198–200. https://doi.org/10.1038/285198a0 (1980).
56. Alvarez, L. W., Alvarez, W., Asaro, F. & Michel, H. V. Extraterrestrial cause for the Cretaceous–Tertiary extinction. *Science* **208**, 1095–1108. https://doi.org/10.1126/science.208.4448.1095 (1980).
57. Roopnarine, P. D. & Angielczyk, K. D. Community stability and selective extinction during the Permian–Triassic mass extinction. *Science* **350**, 90–93. https://doi.org/10.1126/science.aab1371 (2015).
58. Schulte, P. et al. The chicxulub asteroid impact and mass extinction at the Cretaceous–Paleogene boundary. *Science* **327**, 1214–1218. https://doi.org/10.1126/science.1177265 (2010).
59. Chiarenza, A. A. et al. Asteroid impact, not volcanism, caused the end-Cretaceous dinosaur extinction. *Proc. Natl. Acad. Sci.* **117**, 17084–17093. https://doi.org/10.1073/pnas.2006087117 (2020).
60. García-Girón, J. et al. Shifts in food webs and niche stability shaped survivorship and extinction at the end-Cretaceous. *Sci. Adv.* **8**, eadd5040. https://doi.org/10.1126/sciadv.add5040 (2022).
61. Cerezer, F. O. et al. Accelerated body size evolution in upland environments is correlated with recent speciation in South American freshwater fishes. *Nat. Commun.* **14**, 6070. https://doi.org/10.1038/s41467-023-41812-7 (2023).
62. Sambrook, J., Fritsch, E. & Maniatis, T. *Molecular Cloning: A Laboratory Manual*. (Plainview, 1989).
63. Dierckxsens, N., Mardulyn, P. & Smits, G. NOVOPlasty: De novo assembly of organelle genomes from whole genome data. *Nucleic Acids Res.* **45**, e18. https://doi.org/10.1093/nar/gkw955 (2017).
64. Wick, R. R., Judd, L. M., Gorrie, C. L. & Holt, K. E. Unicycler: Resolving bacterial genome assemblies from short and long sequencing reads. *PLOS Comput. Biol.* **13**, e1005595. https://doi.org/10.1371/journal.pcbi.1005595 (2017).
65. Soorni, A., Haak, D., Zaitlin, D. & Bombarely, A. Organelle_pba, a pipeline for assembling chloroplast and mitochondrial genomes from PacBio DNA sequencing data. *BMC Genomics* **18**, 49. https://doi.org/10.1186/s12864-016-3412-9 (2017).
66. Li, H. & Durbin, R. Fast and accurate short read alignment with burrows-wheeler transform. *Bioinformatics* **25**, 1754–1760 (2009).
67. Quinlan, A. R. & Hall, I. M. Bedtools: A flexible suite of utilities for comparing genomic features. *Bioinformatics* **26**, 841–842 (2010).
68. Iwasaki, W. et al. MitoFish and MitoAnnotator: A mitochondrial genome database of fish with an accurate and automatic annotation pipeline. *Mol. Biol. Evol.* **30**, 2531–2540. https://doi.org/10.1093/molbev/mst141 (2013).
69. Bernt, M. et al. MITOS: Improved de novo metazoan mitochondrial genome annotation. *Mol. Phylogenet. Evol.* **69**, 313–319. https://doi.org/10.1016/j.ympev.2012.08.023 (2013).
70. Lowe, T. M. & Chan, P. P. tRNAscan-SE On-line: Integrating search and context for analysis of transfer RNA genes. *Nucleic Acids Res.* **44**, W54–W57. https://doi.org/10.1093/nar/gkw413 (2016).
71. Kerpedjiev, P., Hammer, S. & Hofacker, I. L. Forna (force-directed rna): Simple and effective online rna secondary structure diagrams. *Bioinformatics* **31**, 3377–3379 (2015).

72. Grigoriev, A. Analyzing genomes with cumulative skew diagrams. *Nucleic Acids Res.* **26**, 2286–2290. https://doi.org/10.1093/nar/26.10.2286 (1998).
73. Edgar, R. C. MUSCLE: Multiple sequence alignment with high accuracy and high throughput. *Nucleic Acids Res.* **32**, 1792–1797. https://doi.org/10.1093/nar/gkh340 (2004).
74. Kumar, S., Stecher, G., Li, M., Knyaz, C. & Tamura, K. MEGA X: Molecular evolutionary genetics analysis across computing platforms. *Mol. Biol. Evol.* **35**, 1547–1549. https://doi.org/10.1093/molbev/msy096 (2018).
75. Shen, W., Le, S., Li, Y. & Hu, F. SeqKit: A cross-platform and ultrafast toolkit for FASTA/Q file manipulation. *PLoS ONE* **11**, e0163962. https://doi.org/10.1371/journal.pone.0163962 (2016).
76. Suyama, M., Torrents, D. & Bork, P. PAL2NAL: Robust conversion of protein sequence alignments into the corresponding codon alignments. *Nucleic Acids Res.* **34**, W609–W612. https://doi.org/10.1093/nar/gkl315 (2006).
77. Minh, B. Q. et al. IQ-TREE 2: New models and efficient methods for phylogenetic inference in the genomic era. *Mol. Biol. Evol.* **37**, 1530–1534. https://doi.org/10.1093/molbev/msaa015 (2020).
78. Li, C., Lu, G. & Ortí, G. Optimal data partitioning and a test case for ray-finned fishes (Actinopterygii) based on ten nuclear loci. *Syst. Biol.* **57**, 519–539. https://doi.org/10.1080/10635150802206883 (2008).
79. Pagel, M. & Meade, A. A phylogenetic mixture model for detecting pattern-heterogeneity in gene sequence or character-state data. *Syst. Biol.* **53**, 571–581. https://doi.org/10.1080/10635150490468675 (2004).
80. Pagel, M. & Meade, A. Bayesian analysis of correlated evolution of discrete characters by reversible-jump Markov chain Monte Carlo. *Am. Nat.* https://doi.org/10.1086/503444 (2006).
81. Rambaut, A., Drummond, A. J., Xie, D., Baele, G. & Suchard, M. A. Posterior summarization in Bayesian phylogenetics using tracer 1.7. *Syst. Biol.* **67**, 901–904. https://doi.org/10.1093/sysbio/syy032 (2018).
82. Duan, Y. et al. Bacteriophages against cytolytic *Enterococcus faecalis* as therapy for alcoholic liver disease. *Nature* **6**, 66 (2024).
83. Sakamoto, T. & Ortega, J. M. *TaxOnTree: A tool that generates trees annotated with taxonomic information*. https://doi.org/10.1101/2020.12.24.424364 (2020).
84. Rambaut, A. Figtree v1.4.4 (2018). http://tree.bio.ed.ac.uk/software/figtree/.
85. Letunic, I. & Bork, P. Interactive tree of life (iTOL): An online tool for phylogenetic tree display and annotation. *Bioinformatics* **23**, 127–128. https://doi.org/10.1093/bioinformatics/btl529 (2007).
86. Santini, F., Harmon, L. J., Carnevale, G. & Alfaro, M. E. Did genome duplication drive the origin of teleosts? A comparative study of diversification in ray-finned fishes. *BMC Evol. Biol.* **9**, 194. https://doi.org/10.1186/1471-2148-9-194 (2009).
87. Chen, W.-J., Lavoué, S. & Mayden, R. L. Evolutionary origin and early biogeography of otophysan fishes (Ostariophysi: Teleostei). *Evolution* **67**, 2218–2239. https://doi.org/10.1111/evo.12104 (2013).
88. Near, T. J. et al. Resolution of ray-finned fish phylogeny and timing of diversification. *Proc. Natl. Acad. Sci.* **109**, 13698–13703. https://doi.org/10.1073/pnas.1206625109 (2012).
89. Saitoh, K., et al. Evidence from mitochondrial genomics supports the lower Mesozoic of South Asia as the time and place of basal divergence of cypriniform fishes (Actinopterygii: Ostariophysi). *Zool. J. Linn. Soc.* **161**, 633–662. https://doi.org/10.1111/j.1096-3642.2010.00651.x (2011).
90. Peng, Z., He, S., Wang, J., Wang, W. & Diogo, R. Mitochondrial molecular clocks and the origin of the major Otocephalan clades (Pisces: Teleostei): A new insight. *Gene* **370**, 113–124. https://doi.org/10.1016/j.gene.2005.11.024 (2006).
91. Nakatani, M., Miya, M., Mabuchi, K., Saitoh, K. & Nishida, M. Evolutionary history of Otophysi (Teleostei), a major clade of the modern freshwater fishes: Pangaean origin and Mesozoic radiation. *BMC Evol. Biol.* **11**, 177. https://doi.org/10.1186/1471-2148-11-177 (2011).
92. Benton, M. J. et al. Constraints on the timescale of animal evolutionary history. *Palaeontol. Electron.* **18**(1), 1–106. https://doi.org/10.26879/424 (2015).
93. Gayet, M. & Otero, O. Analyse de la palÃ©odiversification des Siluriformes (Osteichthyes, Teleostei, Ostariophysi). *Geobios* **32**, 235–246. https://doi.org/10.1016/S0016-6995(99)80037-0 (1999).
94. Sytchevskaya, E. Y. Paleogene freshwater fish fauna of the USSR and Mongolia. *Trans. Joint Sov. Mong. Paleontol. Exped.* **66**, 1–157 (1986).
95. Divay, J. D. & Murray, A. M. The fishes of the Farson Cutoff Fishbed, Bridger Formation (Eocene), greater Green River Basin, Wyoming, U. S. A. *J. Vertebrate Paleontol.* **36**, e1212867. https://doi.org/10.1080/02724634.2016.1212867 (2016)
96. Gayet, M. & Meunier, F. J. Paleontology and palaeobiogeography of catfishes. *Catfishes* **2**, 492–522 (2003).

Acknowledgements

We would like to thank the teams from Bioinformatics Multidisciplinary Environment (BioME/IMD) at UFRN, Centro de Processamento de Alto Desempenho (CEPAD/ICB) at UFMG, and High-Performance Computing Center (NPAD) at UFRN for the support on the computational resource.

Author contributions

A.R.S., S.S., S.J.S., J.E.S.S., T.S., Conceptualization; R.L.D.C., C.S.S., A.F.V., E.P., G.L.N., L.F.A.M., G.O., methodology; R.L.D.C., J.E.S.S., T.S., formal analysis; R.L.D.C., T.S., data curation; R.L.D.C., T.S., writing-original draft preparation; A.R.S., S.S., S.J.S., J.E.S.S., T.S., writing-review and editing; A.R.S., S.S., J.E.S.S., T.S., supervision; G.O., A.R.S., S.S., S.J.S., funding acquisition. All authors have read and agreed to the published version of the manuscript.

Funding

This study was financed in part by Coordenação de Aperfeiçoamento de Pessoal de Nível Superior (CAPES, Brazil)—Finance Code 001, and by Instituto Tecnológico Vale (ITV, Brazil). R.L.D.C. received PhD scholarship from Conselho Nacional de Desenvolvimento Científico e Tecnológico (CNPq, Brazil), process no. 141945/2020-6. A.R.S. is supported by CNPq/Brazil with Produtividade (304413/2015-1), by CAPES/BioComputacional, and by Pró-Reitoria de Pesquisa e Pós-Graduação of Federal University of Pará (PROPESP/UFPA). A.F.V., E.P., G.L.N., and G.O. are supported by ITV.

Declarations

Competing interests

The authors declare no competing interests.

Additional information

Supplementary Information The online version contains supplementary material available at https://doi.org/10.1038/s41598-025-94272-y.

Correspondence and requests for materials should be addressed to T.S.

Reprints and permissions information is available at www.nature.com/reprints.

Publisher's note Springer Nature remains neutral with regard to jurisdictional claims in published maps and institutional affiliations.